Proc. Natl. Acad. Sci. USA
Vol. 93, pp. 9477–9482, September 1996
Biochemistry

An RNA topoisomerase

(molecular topology/RNA knot/strand passage)

HUI WANG*, RUSSELL J. DI GATE†, AND NADRIAN C. SEEMAN*‡

*Department of Chemistry, New York University, New York, NY 10003; and †Department of Pharmaceutical Science, School of Pharmacy and Medical Biotechnology Center, University of Maryland Biotechnology Institute, Baltimore, MD 21201

Communicated by Nicholas R. Cozzarelli, University of California, Berkeley, CA, June 6, 1996 (received for review December 22, 1995)

ABSTRACT **A synthetic strand of RNA has been designed so that it can adopt two different topological states (a circle and a trefoil knot) when ligated into a cyclic molecule. The RNA knot and circle have been characterized by their behavior in gel electrophoresis and sedimentation experiments. This system allows one to assay for the existence of an RNA topoisomerase, because the two RNA molecules can be interconverted only by a strand passage event. We find that the interconversion of these two species can be catalyzed by *Escherichia coli* DNA topoisomerase III, indicating that this enzyme can act as an RNA topoisomerase. The conversion of circles to knots is accompanied by a small amount of RNA catenane generation. These findings suggest that strand passage must be considered a potential component of the folding and modification of RNA structures.**

The role of type I topoisomerases (1) is key in the cellular metabolism of DNA. These enzymes are involved intimately in replication, in transcription, and in the maintenance of torsional stress in the genome. The importance of RNA within the cell is well-recognized, as mRNA, as tRNA, in ribosomes, and in processing roles. RNA molecules that have been characterized by x-ray crystallography to high resolution contain hairpins and pseudoknots (2–4). The linear single-stranded character of cellular RNA has generally led to the assumption that functional RNA structures can be achieved without the requirement for strand passage activities to solve problems in RNA molecular topology. Hence, in contrast to DNA, the cellular need for an RNA topoisomerase has not seemed compelling. Nevertheless, it has been shown recently that *Escherichia coli* DNA topoisomerase III (topo III) (5, 6) is capable of cleaving RNA molecules to produce a protein-RNA adduct (7). Here, we demonstrate that topo III is capable of catalyzing strand passage operations that interconvert synthetic RNA circles and knots.

Previously, we have constructed DNA knots by cyclizing synthetic single-stranded molecules using a pairing motif of the form **X-S-Y-S-X′-S-Y′-S-**, where **X** and **Y** represent 11 or 12 nucleotides, respectively, **X′** and **Y′** are their Watson–Crick complements, and **S** is a single-stranded spacer region consisting of dT_n, where n ranges from 6 to 15 (8–12). Knots formed from this motif are typically trefoil knots with negative nodes. However, by using sequences in the **X** or **Y** domains capable of forming left-handed Z-DNA (13), we have also been able to form figure eight knots (9, 10) that are topological rubber gloves (11), as well as trefoil knots with positive nodes (12). We have demonstrated recently that these 104 nt DNA knots and their corresponding circle can be interconverted by *E. coli* DNA topoisomerase I (topo I) and by topo III (14). We have used the same motif to construct a 104-nt RNA trefoil knot, with negative nodes. Fig. 1 illustrates the principles of both knot and circle formation; knot ligations require a 16-deoxynucleotide single-stranded linker and circle formation is promoted by the presence of a 40-deoxynucleotide linker whose binding is incompatible with knot formation. We have used these substrates to demonstrate the RNA strand passage activity of topo III.

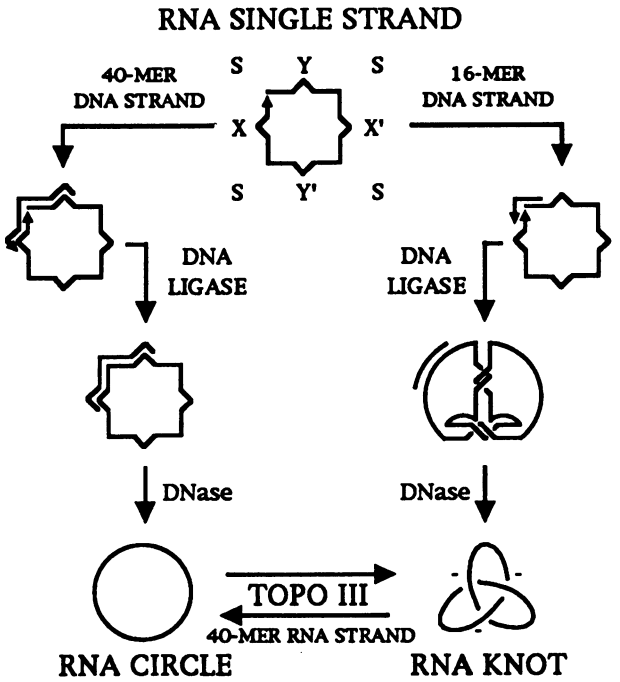

FIG. 1. The synthetic and strand passage reactions performed in this paper. The initial RNA single strand is shown at the top of this diagram. Its Watson–Crick pairing regions, **X**, **Y**, **X′**, and **Y′**, are illustrated as bumps on the square; the spacers denoted by **S** are shown as the corners of the square. The arrowhead denotes the 3′ end of the strand. The pathway to the left illustrates formation of the RNA circle. A 40-nt DNA linker (incompatible with knot formation) is annealed to the molecule, and it is ligated together to form an RNA circle, which survives treatment with DNase. In the other pathway, a 16-nt linker is used in the same protocol to produce the RNA trefoil knot, whose three negative nodes are indicated. The interconversion of the two species by topo III is shown at the bottom. The 40-mer RNA strand promotes the formation of the circle from the knot.

MATERIALS AND METHODS

Preparation of RNA Molecules. The RNA single strand was generated by transcription of T7 RNA polymerase from a DNA strand synthesized on an Applied Biosystems model 380B DNA synthesizer by phosphoramidite procedures (15). Templates were prepared by annealing a short complement to the promoter region of a 131-nt DNA strand containing a 104-nt transcribing region and a 17-nt promoter, preceded by

The publication costs of this article were defrayed in part by page charge payment. This article must therefore be hereby marked "*advertisement*" in accordance with 18 U.S.C. §1734 solely to indicate this fact.

Abbreviations: topo III, topoisomerase III; 2D, two dimensional.

‡To whom reprint requests should be addressed.

10 nucleotides (16). The sequence of the RNA molecule has been designed using the program SEQUIN (17) to minimize the probability of ribozyme formation and RNA polymerase dissociation (18). RNA strands were transcribed (19) using the MEGAshortscript T7 kit (Ambion) that was modified to contain double the usual concentration of uridine triphos-

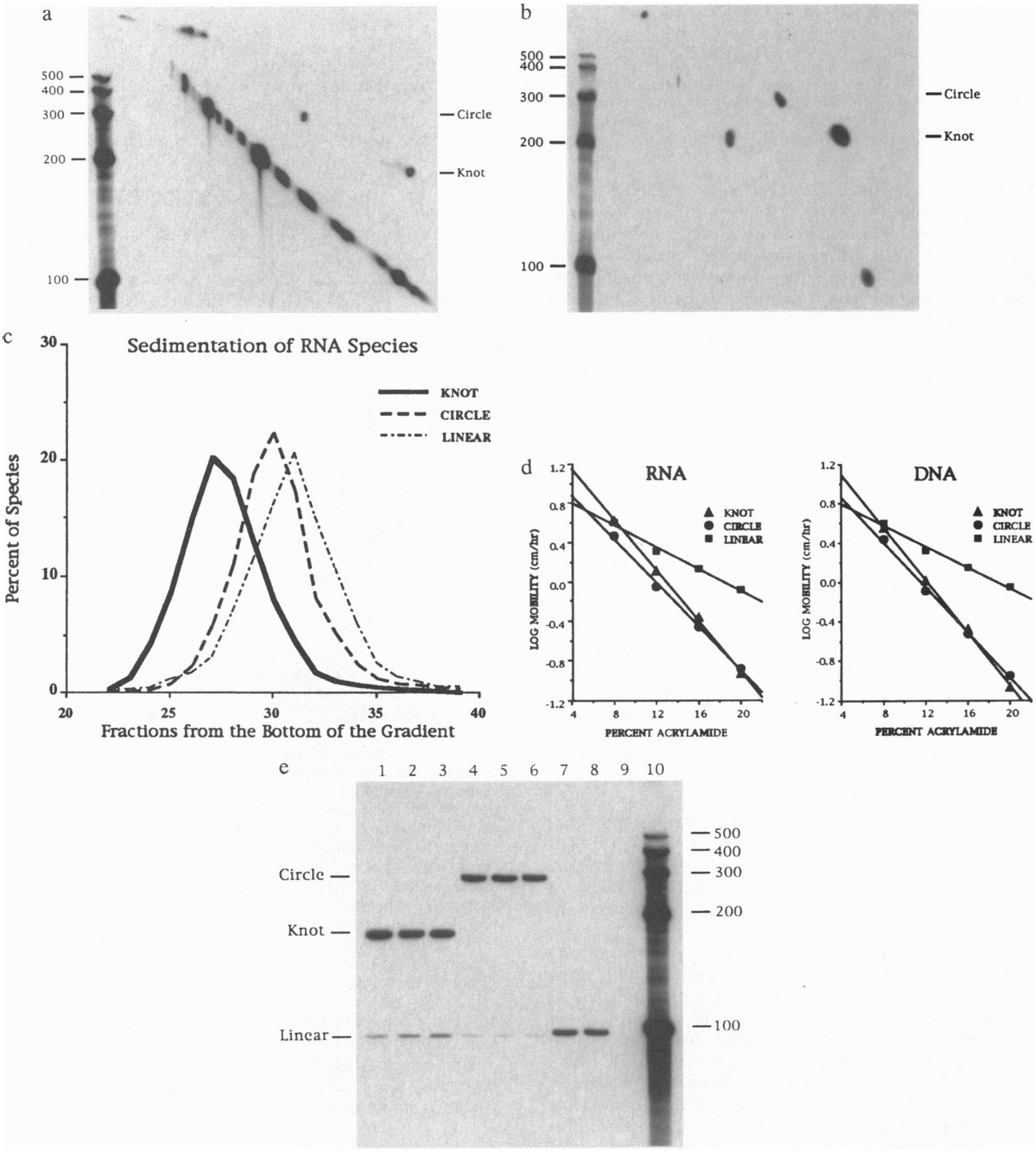

FIG. 2. (*a*) Proof of knot synthesis products of the RNA synthetic reaction. This 2D (8% → 12%) denaturing polyacrylamide gel illustrates the synthesis of both knot and circle. Linear RNA markers have been run in the second direction. The knot is the favored closed species under the conditions of ligation. The off-diagonal spots in the upper-left corner have not been characterized. (*b*) Products of the DNA synthetic reaction. The gel percentages and markers are the same as those in *a*. (*c*) Sedimentation analysis of the products of the synthetic reaction. The three species of RNA are shown. It is clear that the putative knot migrates more rapidly than the circle, which, in turn, migrates more rapidly than the linear molecule. (*d*) Ferguson plots of knotted, circular, and linear RNA and DNA molecules. The two plots indicate that the RNA and DNA species behave similarly. (*e*) DNase I and alkaline phosphatase assays. This autoradiogram of a 12% denaturing gel shows knotted (lanes 1–3), circular (lanes 4–6), and linear (lanes 7–9) RNA molecules; lane 10 contains linear RNA markers. Each lane contains 3 fmol of RNA; digestions proceed for 45 min at 37°C. Lanes 1, 4, and 7 are untreated controls; lanes 2, 5, and 8 show each species treated with 7 units of DNase I. The DNase resistance indicates that no DNA from the transcription or ligation mixture is included within the molecules. The material in lanes 3, 6, and 9 has been treated with 1 unit calf intestine alkaline phosphatase. Knots and circles and their linear (randomly cleaved) breakdown products retain their 5′-labeled phosphates, whereas the linear molecule loses its label.

phate. The transcription reaction was treated with 14–20 units of DNase I (Pharmacia) and 10 units of calf intestine alkaline phosphatase (Pharmacia) at 37°C for 2 hr. The reaction was extracted with phenol/chloroform and precipitated by ethanol; the phosphatase, extraction, and precipitation were repeated to ensure complete removal of 5′ phosphates. RNA was purified on a 10% polyacrylamide denaturing gel and then eluted. The RNA sequence is 5′-GAGGCUCUUU.CUCAGGUCCA.GUCUUUCUUU.CUUUCGUCAG.ACGGAUCUUU.CUUUCUUUCG.ACUGGACCUG.AUUUCUUUCU.UUCGAUCCGU.CUGACUUUCU.UGAU-3′.

Synthesis of Knots. *RNA knot.* RNA strands (50–60 pmol) were labeled with [γ-^{32}P]ATP using 10 units T4 polynucleotide kinase. Ligation was performed in 2–4 μM reactions in the presence of a 16-nt DNA linker molecule in twofold excess. For efficient generation of circles, a DNA linker 40 nt long was used. The ligation conditions used were: 1 unit T4 polynucleotide DNA ligase per μl of reaction mixture, 10% PEG 400, 66 mM Tris·HCl (pH 7.6), 6.6 mM $MgCl_2$, 10 mM DTT, and 66 μM ATP at 16°C for 8–14 hr. Ligation reactions were treated with DNase I before purification on two-dimensional (2D) denaturing gels (8% first dimension; 12% second dimension), followed by phenol/chloroform extraction (once) and chloroform extraction (twice).

DNA knot. The DNA knot was synthesized by the same procedure as the RNA knot, except that enzyme and DNA concentrations were 10-fold lower and PEG 400 was not added to the ligation solution.

2D Gel Electrophoresis. All gels contained acrylamide/bisacrylamide in a ratio of 19:1, 50% urea, and a buffer consisting of 89 mM boric acid, 89 mM Tris (pH 8.3 at 25°C), and 2 mM EDTA. The sample was run on an 8% polyacrylamide gel. Each lane was then excised and run on a 12% denaturing polyacrylamide gel in a second dimension. Before loading onto gels, the samples were dissolved in a denaturing loading dye containing 90% formamide and 5 mM EDTA and heated at 90°C for 3 min. Gels were run at 50–55°C at 31 V/cm.

Ferguson Plots. Absolute mobilities (centimeters per hour) of denaturing gels run at 55°C were measured for Ferguson analysis; logarithms were taken to base 10.

RNA Sedimentation. *Ca.* 50 fmol of each RNA species was denatured by heating in 100 μl of a solution containing 85% formamide and 5 mM EDTA for 5 min at 90°C, followed by quenching in ice. The solution was overlaid on 4 ml of a 3–18% sucrose gradient containing 85% formamide and 5 mM EDTA (20). Sedimentation was performed at 48 krpm for 25.5 hr at 5°C. The radioactive fractions were ethanol precipitated in the presence of 3 μg of tRNA and were electrophoresed on a 12% denaturing gel. The distribution of each species was quantitated using a Bio-Rad model GS-250 Molecular Imager.

Topo III Conversion Reactions. Topo III was prepared as described (21). RNA (20 fmol) was denatured at 90°C for 5 min in 40 mM Tris·HCl (pH 7.5), 20 mM KCl, 1 mM EDTA, and 5 mM $MgCl_2$. The circles were cooled slowly to room temperature and the knots were brought directly to room temperature. The RNA knots were denatured and annealed in the presence of an equimolar amount of a 40-nt RNA complement that discourages knot formation. PEG400 was then added to the mixture to 10% final concentration and 4.5 pmol of topo III was added to the reactions to yield a final volume of 10 μl. The control reactions are incubated with the topo III dilution buffer instead. The topo III dilution buffer consisted of 50 mM Tris·HCl (pH 7.5 at 25°C), 50 mM NaCl, 1 mM DTT, 1 mM EDTA, 50% glycerol, and 0.5 mg/ml BSA. The reactions were carried out at 37°C for 3.5 hr. The reactions were terminated by adding 100 μl of a solution containing 20 mM Tris·HCl (pH 8), 1 mM EDTA, 0.1% SDS, and 1.8 units of proteinase K. This mixture was incubated at 37°C for 1 hr and terminated by phenol/chloroform extraction, which was followed by ethanol precipitation with 6 μg of tRNA as carrier. The samples were divided into two portions. The first portion was loaded directly onto a 12% denaturing polyacrylamide gel. The second portion was mixed with 5′-labeled linear RNA size markers (Ambion) and run on 8% → 12% 2D denaturing gels.

Temperature and Magnesium Dependence of Strand Passage Activity. The reactions were carried out as described above except that 10 fmol of RNA molecules was used in each individual reaction. The $MgCl_2$ concentrations studied were 0, 5, 10, and 20 mM. Temperature dependence at 16, 37, or 52°C was determined using 5 mM $MgCl_2$. All reactions were terminated after 3.5 hr at 37°C by proteinase K digestion and phenol/chloroform extraction. The samples were ethanol precipitated with 6 μg of tRNA as carrier and were run on 12% denaturing gels. The bands were quantitated with a Bio-Rad model GS-250 Molecular Imager.

RESULTS

Synthesis and Characterization of the RNA Knot and Circle. Fig. 2*a* is a 2D denaturing gel illustrating the products of the ligation reaction in the presence of the 16-deoxynucleotide linker; cyclic species run above the diagonal (22). The knot is the dominant closed product, and the circle is a lesser product (*ca.* 5:1); of kinased species, about 50% of the molecules ligate to form linear dimers and 10% form knots. Their relative electrophoretic mobilities are similar to those of DNA species of the same topology and corresponding sequence (Fig. 2*b*). The RNA knot is trailed characteristically by small satellite bands (5–15% of the main band) that represent differently denatured conformers of the knot; material in the main knot band can be converted to material in the satellite bands by extra denaturing treatments. The mobility of the DNA knot is most similar to that of the RNA knot satellites.

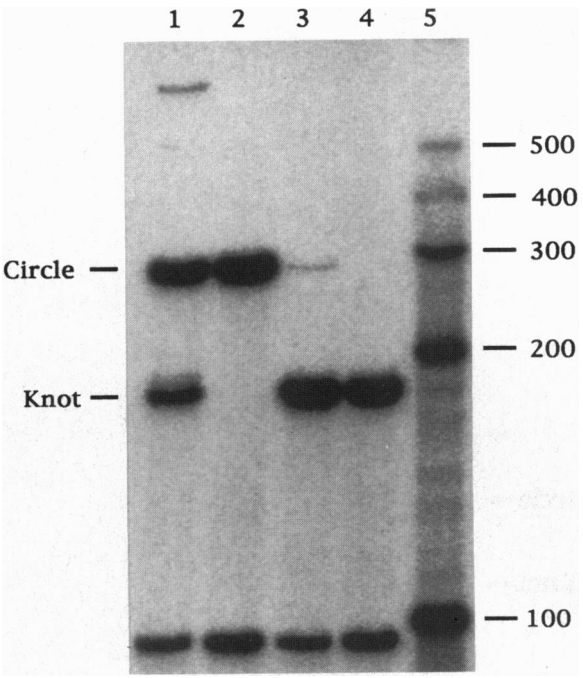

FIG. 3. RNA strand passage catalyzed by *E. coli* DNA topo III. This is a Bio-Rad GS-250 Molecular Imager visualization of a 12% denaturing polyacrylamide gel. Lanes 1 and 2 illustrate the conversion of RNA circle to knot; lanes 3 and 4 illustrate the conversion of RNA knot to circle. Lane 2 contains untreated RNA circles; lane 1 contains RNA circles treated with topo III; lane 4 contains untreated RNA knot; lane 3 contains RNA knots treated with topo III. Note the presence of a small amount of slowly migrating product in lane 1. Lane 5 contains a ladder of RNA markers. All lanes contain linear breakdown products of cyclic molecules.

A further faint band, previously suggested to be a 5_2 knot (8), is visible on original autoradiograms of Fig. 2 *a* and *b*. Fig. 2*c* shows a denaturing sedimentation experiment involving linear, circular, and knotted species. As seen previously with DNA (8), the RNA knot sediments more rapidly than the RNA circle, which, in turn, sediments more rapidly than linear RNA. Fig. 2*d* illustrates Ferguson plots for the RNA and DNA species produced here; slope of a Ferguson plot is proportional to the friction constant of the molecule (23). The similarities between the two plots support the topological assignments we suggest. Fig. 2*e* shows experiments on 5′-end-labeled knotted, circular, and linear molecules, demonstrating that the knot and circle are DNase resistant, and therefore contain no DNA residues. Phosphatase treatment experiments in the same gel show that the 5′ phosphates of the knot and the circle are unavailable, thus confirming the cyclic nature of the knotted and circular molecules. The material in lanes 3, 6, and 9 of Fig. 2*e* has been treated with calf intestine alkaline phosphatase. The cyclic knots and circles retain their (originally) 5′-labeled phosphates. Likewise, their linear breakdown products retain their labels because they are randomly cleaved; fewer than 1% of the linear breakdown molecules are expected to have labeled phosphates available for removal by the phosphatase. By contrast, the linear molecule is seen to lose its label. The knot does not appear to be a substrate for yeast lariat debranching enzyme (24), indicating that it is not a lariat (data not shown).

The Strand Passage Reaction Catalyzed by Topo III. The strand passage reaction is shown schematically at the bottom of Fig. 1. The equilibrium favoring the knot can be shifted slightly to favor a greater proportion of circle by the addition of a long RNA linker, whose pairing with the knot is much less favorable than its pairing with the circle. Fig. 3 shows a denaturing gel containing both interconversions. All lanes contain 10% polyethylene glycol (PEG 400), whose presence fosters the reaction (data not shown). Lane 2 shows an untreated circle control, lane 1 contains circle treated with topo III, lane 4 contains an untreated knot control, and lane 3 shows knot treated with topo III. In each case, the interconversions are evident, although the conversion of the circle to the knot in lane 1 is seen to be favored substantially over the conversion of the knot to the circle in lane 3. A lower mobility product band is also visible in lane 1, but it is not seen in lane 3. Incubation of linear RNA molecules with topo III leads to neither circles nor knots. Likewise, incubation of circles or knots with the topo III dilution buffer produces no interconversion of species. The products have been treated with proteinase K to ensure that there is no protein attached to the RNA. This gel also shows that a fair amount of the cyclic RNA breaks down spontaneously to yield linear molecules.

These reactions are seen more dramatically on 2D gels. Fig. 4 illustrates this point. The conversion of circle to knot is illustrated in the top two panels. On the left, the circle is an off-diagonal spot that is seen to convert to knot on the right. In addition, a small amount of the higher product (Fig. 3, lane 1) is seen off-diagonal in the upper right. Its off-diagonal character demonstrates that it is a cyclic species. When it is heated in a gel, allowed to break down, and then electropho-

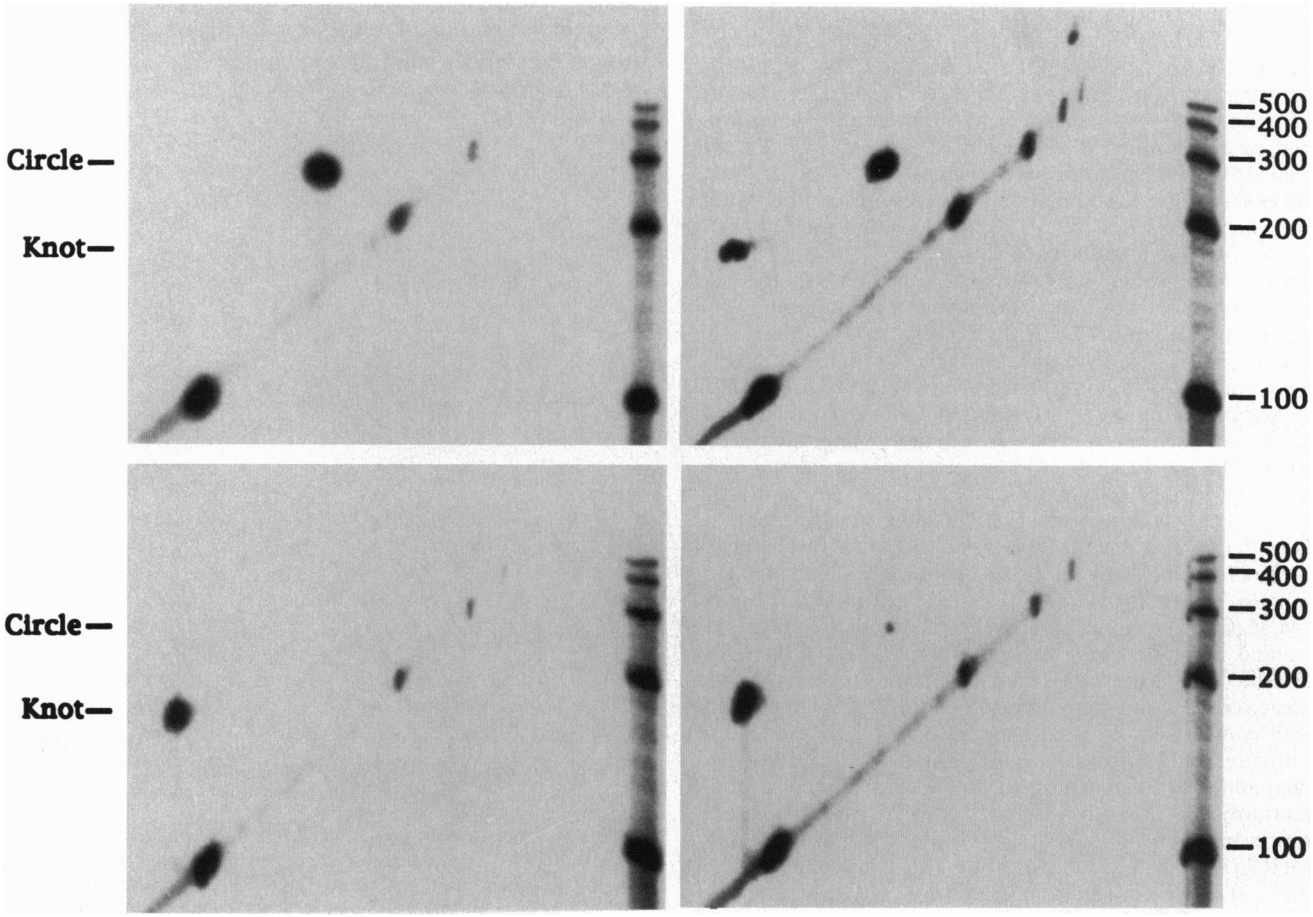

FIG. 4. 2D gels showing the interconversion of RNA knots and circles. Markers have been loaded on these (8% → 12% denaturing) gels in each dimension. (*Upper Left*) A circular control, untreated with topo III. (*Upper Right*) The same material treated with topo III and plainly demonstrating the cyclic topology of both the knotted product and the catenated product in the band at the upper right. (*Lower Left*) A knotted control. (*Lower Right*) The same material treated with topo III, again demonstrating that the product is cyclic. Controls here and in Fig. 3 have been incubated with all components of the reaction mixture except for topo III.

resed in a second dimension, the products are a circular molecule and a linear molecule (data not shown). We conclude that it is a circle catenated to a (presumably unknotted) second circle. The lower panels of Fig. 4 illustrate the conversion of the knot to the circle. This reaction is not as strongly favored as the reverse reaction, but the presence of a small amount of circle is nevertheless evident on the gel.

Solution Optima for the Interconversions. We have investigated the interconversions at a series of temperatures and of magnesium concentrations. Amongst magnesium concentrations of 0, 5, 10, and 20 mM, all strand passage reactions (circle to knot, circle to catenane, and knot to circle) were seen to be most effective at a concentration of 10 mM Mg^{2+} (data not shown). Fig. 5 shows the topoisomerizations as a function of temperature. At 16°C, a small amount of circle is converted to knot, but substantial amounts of all products are seen at the physiological temperature of 37°C. The topo III DNA strand passage activity is most active at 52°C (6), and this is also true of the RNA strand passage activity described here.

Identity of the Topoisomerase. We have confirmed that topo III is the active toposiomerase in an experiment using a mutant enzyme, in which catalytic tyrosine-328 is replaced by phenylalanine (25). For this experiment, the native enzyme (topo III-Y) and the mutant (topo III-F) were isolated under the same conditions (25), so that any trace contaminants would be the same in both cases. Fig. 6 illustrates the conversion of RNA circle to knot in reactions catalyzed by stoichiometric mixtures of topo III-Y and topo III-F. It is clear that strand passage is dependent on the presence of topo III-Y (lanes 3–6), that it decreases in proportion to the percentage of topo III-F (lanes 4–6), and that it is absent in the reaction containing exclusively topo III-F (lane 7). The reverse reaction produces similar results (data not shown). These data establish unambiguously that topo III is the enzyme responsible for RNA strand passage. Topo I does not catalyze RNA strand passage when tested under the same conditions as topo III (data not shown).

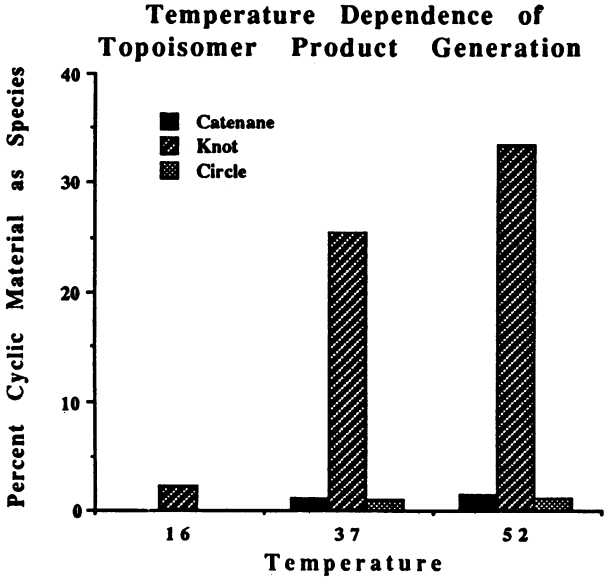

FIG. 5. Temperature dependence of RNA strand passage activity. The products of the strand passage reactions are presented for the three temperatures tested: 16°C, 37°C, and 52°C. The knot and the catenane are produced by using the circle as a substrate, whereas the circle is produced by using the knot as a substrate. The remaining material from each reaction is not shown, but constitutes the rest of the percentage summing to 100%. In addition, about 10% of the starting cyclic material (not counted) breaks down to linear molecules at 16°C and at 37°C, and about 15% breaks down at 52°C.

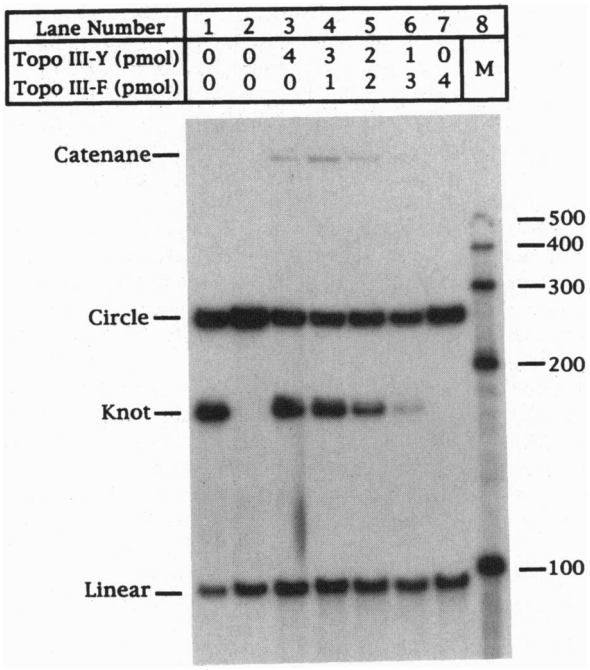

FIG. 6. Strand passage in reactions catalyzed by mixtures of active topo III-Y and inactive topo III-F. Each reaction is treated in the same way as in Figs. 3 and 4 except that 10 fmol of RNA is used for each reaction. Lane 1 contains markers of purified RNA circle, knot, and linear molecules; lane 8 contains linear RNA length markers; lane 2 contains only purified RNA circle incubated with topo III dilution buffer; lanes 3–7 contain, respectively, stoichiometric mixtures of topo III-Y (active) and topo III-F (inactive) in the ratios: 4:0, 3:1, 2:2, 1:3, and 0:4. Quantitation of the material in each lane reveals the following percentages of [circle, knot, catenane, and linear], respectively: lane 2, (0 topo III-Y:0 topo III-F) [87.8, 0.6, 0.0, 11.6]; lane 3, (4:0) [45.5, 25.8, 0.8, 27.9]; lane 4, (3:1) [40.1, 24.0, 1.9, 32.9]; lane 5, (2:2) [54.6, 12.9, 1.75, 30.8]; lane 6, (1:3) [54.5, 5.5, 0.5, 39.5]; lane 7, (0:4) [69.0, 0.0, 0.01, 30.9]. We ascribe the 25–40% linear material to breakdown of the circular species; the large amount seen in lane seven suggests that it is not a protein-RNA adduct. We ascribe the trace of knot detected on quantitation of lane 2 to the presence of very highly radioactive samples in the flanking lanes.

DISCUSSION

The interconversions we have demonstrated require strand passage to occur in closed molecules; thus, topo III is capable of catalyzing RNA strand passage reactions. Topo III has no cofactor to drive the reaction in either direction; the knot is favored in synthesis conditions, so we have added the 40-nt RNA complement to promote conversion to the circle, although it is not absolutely required. The product ratio in synthetic reactions is about 5:1, whereas it is at least 25:1 in strand passage reactions under the same conditions. Indeed, the catenane is produced from the circle via an intermolecular reaction in quantities similar to the amount of circle produced from the knot. It is possible that topo III encounters a steric problem binding to the knot, but not in binding to a circular substrate as seen with topo I in relaxing superhelical DNA (26).

We do not know whether the strand passage noted here occurs within the cell. The RNA strand passage activity is certainly present at the physiological temperature of 37°C, although, like the DNA strand passage activity (6), it is more active at 52°C. Dröge (27) has used the RNase sensitivity of a transcription-driven *in vitro* recombination system to demonstrate that RNA can be involved in a torque-producing structure. The strand passage activity reported here could be used to relieve stress associated with RNA molecules whose ends are fixed.

We have demonstrated clearly that topo III is responsible for the RNA strand passage activity we have uncovered. Mutants lacking topo III are known to demonstrate increased levels of spontaneous deletions (28, 29). The role of an RNA topoisomerase activity in preventing this phenotype is not obvious. Likely intracellular roles for an RNA topoisomerase activity would include facilitation or regulation of RNA folding (30–32) or of transcription (7). The phenotypes of cells known to lack topo III activity do not suggest strongly the lack of RNA topoisomerase activity. However, the characteristics of cells without an RNA strand passage activity are not plainly evident. Likewise, the absence of topo III does not necessarily imply the absence of all RNA strand passage activity, because topo III may not be the only RNA topoisomerase. The findings reported here suggest that topo III and possibly other enzymes are available to catalyze topological aspects of RNA metabolism, just as it and other DNA topoisomerases can participate in modulating DNA linkage. If this activity persists within the cell, strand passage must be considered among the possible mechanisms that establish (33) and modify RNA structure.

We thank Dr. Jef D. Boeke for his generous gift of debranching enzyme and Dr. Yuk-Ching Tse-Dinh for her generous gift of *E. coli* DNA topo I. We are grateful to Dr. Richard P. Cunningham for many valuable suggestions and discussions throughout this work. We thank Dr. David C. Schwartz for his help with the sedimentation experiments. We are also grateful to Drs. Nicholas Cozzarelli, Louise Pape, Deok-Joon Choi, David Scicchitano, William T. McAllister, and Melissa Moore for useful advice on various aspects of the project. This research has been supported by National Institutes of Health Grant GM-29554 to N.C.S. and Grant GM-48445 to R.J.D.G. and by a Margaret and Herman Sokol Fellowship to H.W.

1. Wang, J. C. (1971) *J. Mol. Biol.* **55,** 523–533.
2. Rich, A. & RajBhandary (1976) *Annu. Rev. Biochem.* **45,** 805–860.
3. Pley, H. W., Flaherty, K. M. & McKay, D. B. (1994) *Nature (London)* **372,** 68–74.
4. Scott, W. G., Finch, J. T. & Klug, A. (1995) *Cell* **81,** 991-1002.
5. Dean, F. B., Krasnow, M. A., Otter, R., Matzuk, M. M., Spengler, S. J. & Cozzarelli, N. R. (1982) *Cold Spring Harbor Symp. Quant. Biol.* **47,** 769–777.
6. Srivenugopal, K. S., Lockshon, D. & Morris, D. R. (1984) *Biochemistry* **23,** 1899–1906.
7. Di Gate, R. J. & Marians, K. J. (1992) *J. Biol. Chem.* **267,** 20532–20535.
8. Mueller, J. E., Du, S. M. & Seeman, N. C. (1991) *J. Am. Chem. Soc.* **113,** 6306–6308.
9. Du, S. M. & Seeman, N. C. (1992) *J. Am. Chem. Soc.* **114,** 9652–9655.
10. Wang, H., Du, S. M. & Seeman, N. C. (1993) *J. Biomol. Struct. Dyn.* **10,** 853–863.
11. Flapan, E. & Seeman, N. C. (1995) *J. Chem. Soc. Chem. Commun.* 2249–2250.
12. Du, S. M., Stollar, B. D. & Seeman, N. C. (1995) *J. Am. Chem. Soc.* **117,** 1194–1200.
13. Rich, A., Nordheim, A. & Wang, A. H.-J. (1984) *Annu. Rev. Biochem.* **53,** 791–846.
14. Du, S. M., Wang, H., Tse-Dinh, Y.-C. & Seeman, N. C. (1995) *Biochemistry* **34,** 673–682.
15. Caruthers, M. H. (1985) *Science* **230,** 281–285.
16. Choi, D., Marino-Alexandra, D. J., Geacintov, N. E. & Scicchitano, D. A. (1994) *Biochemistry* **33,** 780–787.
17. Seeman, N. C. (1990) *J. Biomol. Struct. Dyn.* **8,** 573–581.
18. Wyatt, J. R., Chastain, M. & Puglisi, J. (1981) *BioTechniques* **11,** 764–769.
19. Milligan, J. F. & Uhlenbeck, O. C. (1989) *Methods Enzymol.* **180,** 51–62.
20. Rickwood, D. & Chambers, J. A. A. (1984) in *Centrifugation: A Practical Approach*, ed. Rickwood, D. (IRL, Oxford), 2nd Ed., pp. 101–101.
21. Hiasa, H., Di Gate, R. J. & Marians, K. J. (1994) *J. Biol. Chem.* **269,** 2093–2099.
22. Ford, E. & Ares, M., Jr. (1994) *Proc. Natl. Acad. Sci. USA* **91,** 3117–3121.
23. Rodbard, D. & Chrambach, A. (1971) *Anal. Biochem.* **40,** 95–134.
24. Nam, K., Hudson, H. E., Chapman, K. B., Ganeshan, K, Damha, M. J. & Boeke, J. D. (1994) *J. Biol. Chem.* **269,** 20613–20621.
25. Zhang, H. L. & Di Gate, R. J. (1994) *J. Biol. Chem.* **269,** 9052–9059.
26. Kirkegaard, K. & Wang, J. C. (1985) *J. Mol. Biol.* **185,** 625–637.
27. Dröge, P. (1993) *Proc. Natl. Acad. Sci. USA* **90,** 2759–2763.
28. Whoriskey, S. K., Schofield, M. A. & Miller, J. H. (1991) *Genetics* **127,** 21–30.
29. Schofield, M. A., Agbunag, R., Michaels, M. L. & Miller, J. H. (1992) *J. Bacteriol.* **174,** 5168–5170.
30. Tsuchihashi, Z., Khosla, M. & Herschlag, D. (1993) *Science* **262,** 99–102.
31. Herschlag, D., Khosla, M., Tsuchihashi, Z. & Karpel, R. L. (1994) *EMBO J.* **13,** 2913–2924.
32. Coetzee, T., Herschlag, D. & Belfort, M. (1994) *Genes Dev.* **8,** 1575–1588.
33. Draper, D. (1996) *Trends Biochem. Sci.* **21,** 145–149.